# Gravity–magnetic appraisal at the interface of Cuddapah Basin and Nellore Schist Belt (NSB) for shallow crustal architecture and tectonic settings

SHUVA SHANKHA GANGULI[1], SANJIT KUMAR PAL[2,*] , J V RAMA RAO[1] and B SUNDER RAJ[1]

[1]*Geological Survey of India, Hyderabad 500 068, India.*
[2]*Department of Applied Geophysics, Indian Institute of Technology (Indian School of Mines), Dhanbad 826 004, India.*
*Corresponding author. e-mail: sanjitism@gmail.com*

Cuddapah Basin (CB) is an intracontinental, Proterozoic basin flanked by Eastern Dharwar Craton (EDC) in the west, Nellore Schist Belt (NSB) and Eastern Ghat Mobile Belt (EGMB) in the east, represents second largest Proterozoic basin of India. Gravity and magnetic surveys were carried out at the interface of Cuddapah Basin (CB) and Nellore Schist Belt (NSB) covering $\sim$2880 km$^2$ area. Gravity map has brought out some distinct zones. The thrusted contact of NSB and Cuddapah sediments has been well delineated from the gravity map by NE–SW trending steep gradient of contours. Relatively high gravity values are observed over NSB in the southeastern part, moderately high values are observed over Cumbum Formation, but distinct low is observed over Baironkonda Formation. These gravity highs and lows are mainly the manifestation of basement characteristics and intrusives. The magnetic map shows two distinct domains, viz., moderate to low zone in the southern part, and moderate to high zone in the northern part. Regional gravity map suggests a change in basement characteristics from felsic to mafic from NW to SE. Presence of mafic basement may be representing EGMB group of rocks underneath the Cuddapah sediments at the eastern part of the study area. The joint gravity and magnetic modelling reveal varied nature of sedimentary units in terms of density and susceptibility and change in basement characteristic.

**Keywords.** Cuddapah Basin; Nellore Schist Belt; gravity–magnetic; regional–residual; joint gravity–magnetic modelling.

## 1. Introduction

Cuddapah Basin (CB) is the largest intra-cratonic basin of southern India, developed over Eastern Dharwar Craton (EDC) after the stabilization of craton at $\sim$2.6–2.5 Ga. It is a Proterozoic basin with an outcrop area of 45,000 km$^2$ (Saha and Patranbis-Deb 2014) and cumulative sedimentary thickness of 10–12 km (Kaila *et al.* 1979), which makes it second largest Proterozoic basin of India (Chetty 2011; Tripathy and Saha 2013). CB is endowed with rich mineral deposit and at the same time, it bears the imprints of the tectonic and physical process that took place from Neo-Archean to Neoproterozoic. Insights regarding the nature of crust, structural fabric, sedimentary nature, and
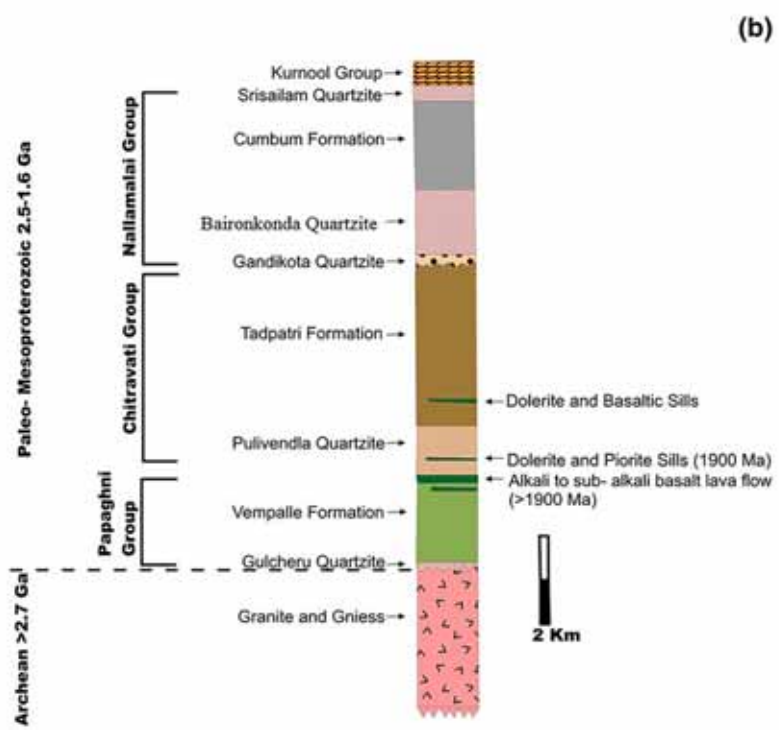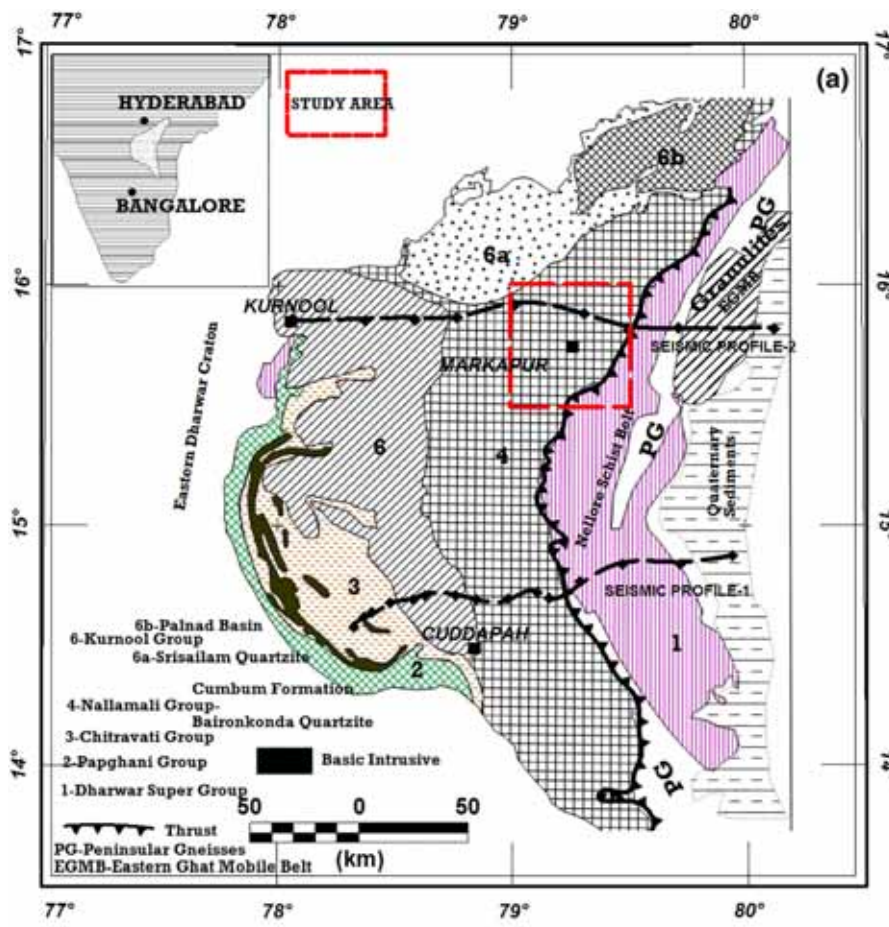
Figure 1. (**a**) Generalized geological map and (**b**) stratigraphy of Cuddapah Basin (modified after Singh and Mishra 2002; Manikyamba *et al.* 2008; Saha and Tripathy 2012).

thickness are of primary importance since it will enhance the understanding of the evolution of CB. The eastern part of the basin (figure 1) is flanked by Nellore Schist Belt (NSB) and granulites of Eastern Ghat Mobile Belt (EGMB). NSB is represented by greenschist to amphibolite facies of metamorphic rock, which are related to subduction magmatism (Dharma Rao and Reddy 2009). Recently, suprasubduction zones comprising ophiolites have also been reported from NSB (Dharma Rao and Reddy 2009). The geophysical study at the interface of CB and NSB provides an opportunity to have an insight of the tectonic process and resultant crustal architecture at the eastern margin of CB.

Gravity–magnetic survey have facilitated the understanding of crustal fabrics and tectonics of Precambrian crust immensely in different parts of the world. Distinct gravity signatures (paired negative and positive gravity anomalies) are observed over cratonic convergence and sutures of Precambrian age in Canadian Shield (Gibb and Thomas 1976; Gibb *et al.* 1983). Suture zones/terrane boundaries in Italy, Canada, Australia, and Africa are reflected as sigma-shaped gravity anomaly (Fountain and Salisbury 1981). The crustal structures across CB and its basement configuration have been primarily derived from gravity studies (Kailasam 1976; Krisna Brahmam 1989; Ram Babu 1993; Kesavamani *et al.* 1997; Singh and Mishra 2002; GSI and NGRI 2006) and seismic studies (Kaila *et al.* 1979; Singh and Mishra 2002; Chandrakala *et al.* 2013). Seismic studies reported huge thickness of sediments ($\sim$10 km) in the Cuddapah basin (Kaila *et al.* 1979; Kaila and Tewari 1985) and identified the underlying Archean basement characterized by the velocity of 6.40 km/s. The studies indicated vertical movement on either boundaries of the CB, which is responsible for huge sediment accumulations ($\sim$10–12 km). These study also indicates that the eastern margin of CB is thrusted below EGMB (Chandrakala *et al.* 2013). The previous geophysical studies (Kaila *et al.* 1979; Kaila and Tewari 1985; Ram Babu 1993; Singh and Mishra 2002; Chandrakala *et al.* 2013) mostly address different aspects of deep crustal fabric and tectonics across CB, but shallow crustal architectures/fabrics are not adequately dealt especially at the eastern margin of CB. At the same time, different schools of thought coexist regarding basin formations and subsequent evolutions.

Present study mainly covers northeastern fringe of CB and a part of NSB. It adopts an integrated approach comprising gravity and magnetic methods with high-density data points to study the (i) shallow basin configuration, (ii) detailed structural fabrics with basement architecture, and (iii) gravity and magnetic signature at the interface of CB and NSB. The objectives are achieved by analysis of the Bouguer gravity map, magnetic anomaly map, their potential transform map, and gravity–magnetic modelling.

## 2. Geological setting

Cudapah basin is evolved over Eastern Dharwar Craton (EDC, Tripathy and Saha 2013). EDC is characterized by gneisses of the granitic composition, which was also affected by the voluminous plutonic intrusion of K-granite of Late Archaean age (Jayananda *et al.* 2000). The CB sediments belonging to Cuddapah Super (CS) Group and Kurnool sequence were collectively deposited from 1900 to 500 Ma and it evolved on the Archean Dharwar craton (Manikyamba *et al.* 2008). The CS Group of rocks representing volcano-sedimentary sequence are composed of argillaceous and arenaceous sequence, subordinate calcareous sediments with both intrusive and extrusive igneous bodies. The general stratigraphy is depicted in figure 1(b) (Murthy 1981). The study area is bounded by longitudes 79°00′–79°30′E and latitudes 15°30′–5°30′N and falls in Survey of India toposheet nos. 57M/1, M/2, M/5 and M/6. The area mostly covers Nallamalai Group of rocks, but south-eastern part of the study area covers Dharwar Super Group/NSB (figures 1 and 2). The rocks of Nallamalai Group are in highly deformed state and comprise of Baironkonda Formation (Quartzite) and Cumbum Formation (slates, phyllites, limestone, etc.).

The large scale regional geo-tectonic features at the eastern part of Cuddapah basin include Nellore Schist Belt (NSB) and Eastern Ghats Mobile Belt (EGMB). The NSB is a curvilinear deformed Paleoproterozoic to Mesoproterozoic volcanosedimentary sequence thrusted over Cuddapah basin (Dharma Rao and Reddy 2009). The Eastern Ghats Mobile Belt, which occurs at eastern flank of NSB, is a high-grade granulite terrane comprising rocks of Archaean to Neoproterozoic age.

The development of Proterozoic Cuddapah Basins (CB) took place after the stabilization of Dharwar Cratonic core at $\sim$2.6–2.5 Ga (Saha *et al.* 2015). The initiation CB was invoked as a broad trough on the Archean basement created in an
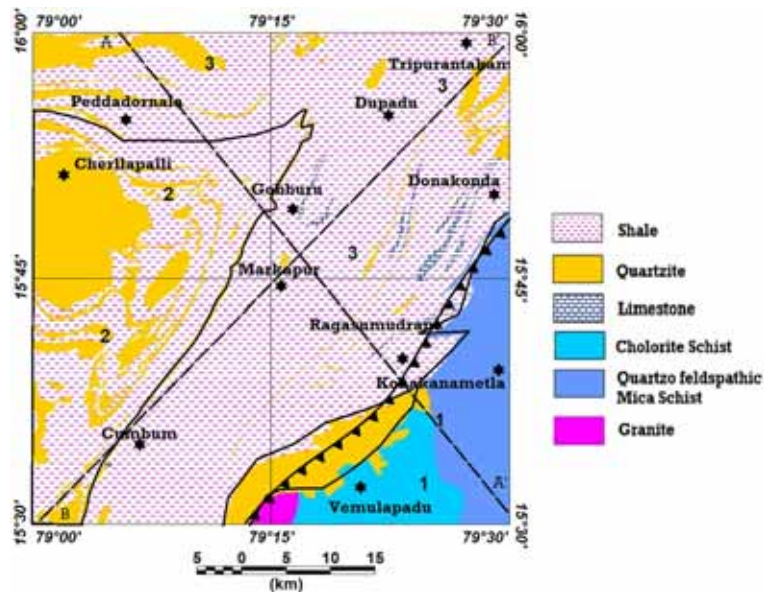
Figure 2. Geological map of the study area. 1: Nellore Schist Belt (NSB); 2: Baironkonda Formation and 3: Cumbum Formation. Profiles A–A′ and B–B′ have been selected for study of gravity–magnetic responses. Gravity–magnetic joint modelling has been carried out along profile A–A′.

extensional regime caused by early Proterozoic thermal activities, as evidenced by mafic–ultra-mafic sill complex (Singh and Mishra 2002; Anand *et al.* 2003). The extensional regime opened an ocean basin at ∼1.89 Ga (Dasgupta *et al.* 2013) over which Cuddapah sediments were deposited. The extensional settings modified into subduction regime and the fold thrust belts at the eastern margin of the Cuddapah basin was formed at ∼1.87 Ga (Saha *et al.* 2010; Dasgupta *et al.* 2013). The possible occurrence of ophiolites within NSB (Dharma Rao and Reddy 2009; Vijay Kumar *et al.* 2010) indicates of convergence of two cratonic blocks (India and East Antarctica, Dobmeier and Raith 2003) in late to middle Proterozoic (Chetty and Murthy 1994) with remnants of ocean basin lying in between. The Eastern Ghats Mobile Belt (EGMB), which was part of East Antarctica Napier Complex accreted and subsequently collided with Indian land mass (Dharwar Craton). The event was culminated at ca. 1.6 Ga (Dasgupta *et al.* 2013).

## 3. Data acquisition and methodology

Gravity and magnetic surveys were carried out alongside all the accessible road and cart tracks in the site covering the Survey of India toposheet Nos. 57M/1, M/1, M/5, and M/6 (figure 3). A total of 1000 gravity magnetic observations were recorded

in 2880 km$^2$ area with station density of one station per 2.8 km$^2$. The elevations have been collected using 'Total Station' survey instrument. The survey strategy was to maintain uniform station distribution throughout the area; however, uniform station distribution was disturbed due to non-approachability in small patches over the reserved forest and rugged hilly terrain. The digital elevation image map of the study area with white dots representing gravity and magnetic stations are shown in figure 3. Gravity base was established near the camp at Markapur (79.26°E, 15.74°N). It was tied with the IGSN-1971 base at Giddalur (78°55′04″, 15°22′28″) established by Geophysics Division, Geological Survey of India (GSI). The CG-5 gravimeter has been used for gravity data acquisition, which has inbuilt software for taking care of tidal correction. After applying drift correction, entire data have also been corrected for free air and Bouguer plate. Bouguer plate correction has been performed assuming the standard crustal density of 2.67 gm/cc. International gravity formula 1980 has been used for latitude correction. The total magnetic field data have been acquired using GSM made Proton Precession Magnetometer. The recorded data have been corrected for diurnal and IGRF (2010, epoch) variation. The overall accuracy of Bouguer gravity and magnetic are in the order of 0.2 mGal and 1 nT, respectively. The corrected data were gridded using minimum
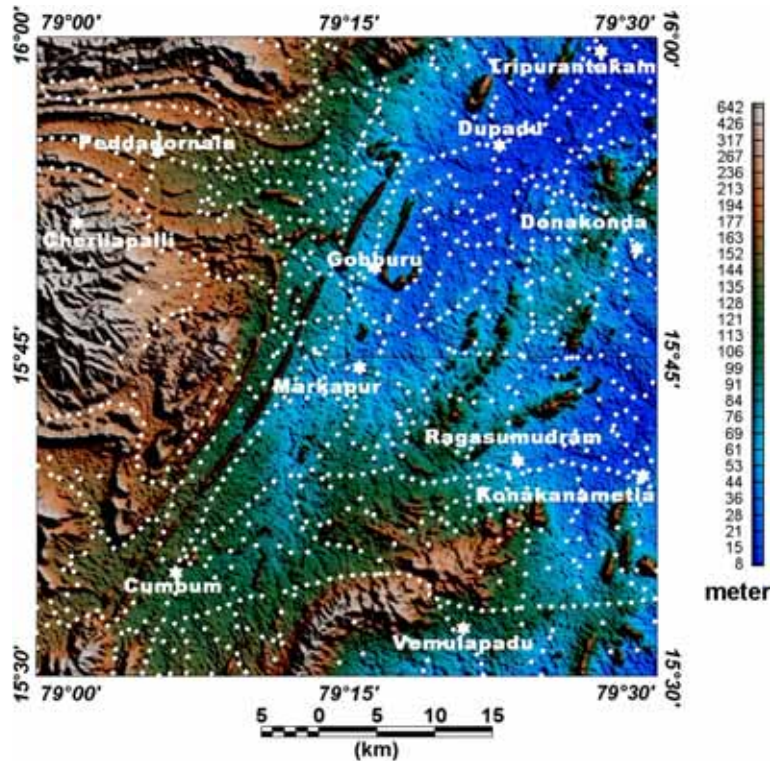
Figure 3. Digital elevation image map of the study area; white dots represent gravity and magnetic stations.

curvature technique with 1000 m grid interval and different filters were applied to assemble the geophysical texture at different crustal level.

Firstly, spectral analysis of both gravity and magnetic data were carried out. Both gravity and magnetic map are the superposition of anomalies of different frequencies caused by sources at different depths. Spectral analysis of the gravity and magnetic data have the efficacy for estimating the average depth of the sources. Spector and Grant (1970) established a simple relation between the power spectrum and depth values of ensembles of uncorrelated magnetic sources from aeromagnetic data and the relationship is expressed as, $P(w) = A\exp(-2|w|h)$, where $P(w)$ is the power spectrum, $A$ is the constant for the randomly distributed source, $w$ is the wavenumber, and $h$ is the depth to the source. After taking logarithm on both sides, the above equation can be written as $\ln(p) = -2|w|h + A$. The plot between the log power spectrum and wavenumber has been used to estimate depth from the slope. The depth of the deeper sources are estimated from slope with smaller wavenumbers. Subsequently, shallower sources are estimated from slopes with higher frequencies.

The horizontal gradient of the gravity data simply indicates the lateral density inhomogeneities (Kumar *et al.* 2018, 2019; Pal and Kumar 2019; Sahoo and Pal 2019; Chouhan *et al.* 2020) and calculated using the formula

$$h(x,y) = \left[\left(\frac{\partial g(x,y)}{\partial x}\right)^2 + \left(\frac{\partial g(x,y)}{\partial y}\right)^2\right]^{1/2},$$

where $h(x, y)$ is the magnitude of horizontal gradient and terms on the parenthesis are the partial derivative of gravity anomaly data with respect to x- and y-axis, respectively. The location of maxima of horizontal gradient magnitude can be simply made by visual inspection. The magnitude of the anomaly depends on density contrast at the boundaries of different litho-units and vertical extension of the contact. The steepest horizontal gradient of a gravity anomaly generally occurs directly over the edge of the body if the edge is vertical (Thomas *et al.* 1992).

The magnetic field is bipolar in nature and the induced magnetic field is a function of latitude, magnetic inclination, and declination (Pal *et al.* 2016, 2017). The Total Intensity Magnetic (TMI) grid was reduced to the equator (RTE) to negate the effect of magnetic inclination on the shape of the anomalies and to centre the anomaly directly over the causative source. Reduction to equator (RTE) is the preferred operation for lower magnetic latitude. It is to be noted that in the case of
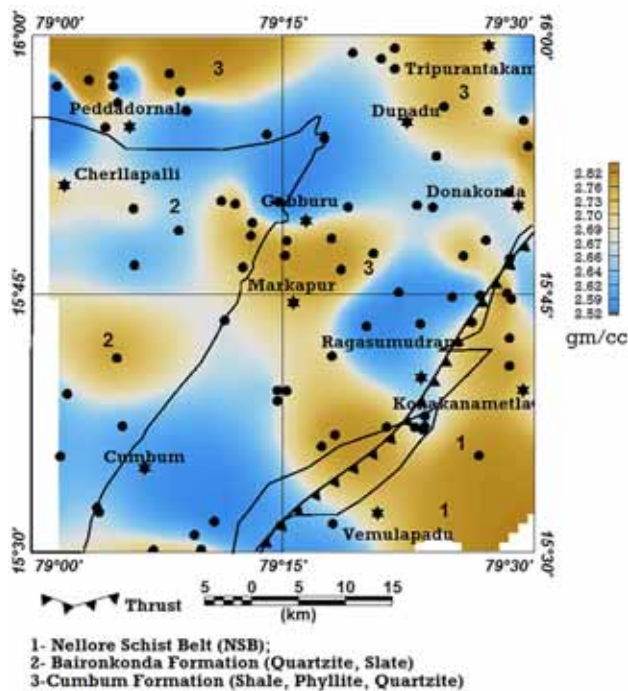
Figure 4. Density map with black dots representing the locations of collected rock samples.

RTE, geomagnetic field is predominantly horizontal. For an induced type of magnetization, the magnetic body near the magnetic equator will oppose the geomagnetic field of the earth and negative (low) anomaly will be recorded (Dobrin and Savit 1988; Mishra 2011). Hence, in general, magnetic low will be observed over magnetic bodies and the magnetic high will be observed over dia and paramagnetic bodies.

A total of 80 rock samples were collected from different representative geological units (figure 4) of the study area. The density and susceptibility of all the samples were measured. The Bartington MS-2 susceptibility meter was used for measuring susceptibility of the samples. Density measurements were carried out with an electronic balance instrument of Afcost make.

## 4. Results

### 4.1 *Physical properties of the rock samples*

The study area is represented by ensembles of litho-units from metasediments to metavolcanics representing Cuddapah formations and NSB, but the physical property of the rock (density and susceptibility) samples are not well documented in the literature. The measured density value of the rock samples has important implications for the analysis of gravity data (Smithson 1971; Subrahmanyam and Verma 1982), since density contrast is the causative source of the gravity anomalies. It facilitates the corroboration of gravity response with the exposed geology. The density and susceptibilities of the representative rock samples from the study area are tabulated in table 1. The table shows that collected rock samples are classified into six lithological units. Representations of high-grade metamorphic rocks like metabasalt or amphibolite are few and sporadic but these rocks are of higher density. The sample representing hematite–quartzite registered the highest density and the sample was collected from the northwestern part of the study area (figure 4). The other sedimentary units like quartzite and limestone are of average density with 2.66 and 2.62 gm/cc, respectively. The previous study shows that the density of Cuddapah sediment varies between 2.5 and 2.7 $gm/cm^3$ (Ram Babu 1993). Singh and Mishra (2002) considered density variation of Cuddapah Formations from 2.60 to 2.81 gm/cc. The present study shows that individual litho-units may have density values that can offshoot the previous estimates.

The susceptibility values of the Cuddapah Formations are not yet reported to the best of our knowledge. However, it has important implications, not only to understand the magnetic anomaly map, but it also facilitates petrological analysis

Table 1. *Measured physical properties of the representative rock samples.*

| Sl. no. | Rock type | No. of samples | Density '*D*' in gm/cc | | Magnetic susceptibility ($S$) range in CGS units ($\times 10^{-6}$) |
|---|---|---|---|---|---|
| | | | Range | Average | |
| 1 | Meta basalt | 08 | 2.67–2.87 | 2.76 | 1–233 |
| 2 | Amphibolite | 04 | 2.69–2.78 | 2.74 | 10–102 |
| 3 | Hematite quartzite | 02 | 2.66–3.03 | | 2–9 |
| 4 | Limestone/Dolomite | 15 | 2.56–2.69 | 2.62 | 1–74 |
| 5 | Quartzite | 31 | 2.6–2.78 | 2.66 | –7.2–6 |
| 6 | Phyllite | 20 | 2.63–2.92 | 2.71 | –4.3–16 |

of the rock samples. The measured rock susceptibilities of the rock sample show that quartzite is of paramagnetic to diamagnetic nature, in general. However, for few samples, it has shown high susceptibility values such as $1310 \times 10^{-6}$ CGS units, $413 \times 10^{-6}$ CGS units, $176 \times 10^{-6}$ CGS units and for all the cases, density values are also in the higher side (2.83, 2.78, and 2.68 gm/cc). It may indicate the presence of a higher percentage of magnetite/ferruginous mineral in the mentioned samples. Limestone dolomites show paramagnetic character. The susceptibility of phyllites varies from $-4.7 \times 10^{-6}$ CGS units to $16.4 \times 10^{-6}$ CGS units except for two samples with susceptibility of $1079.8 \times 10^{-6}$ CGS units (density – 2.92 gm/cc), and $915 \times 10^{-6}$ CGS units (density – 2.78 gm/cc). Metabasalts records moderate susceptibility value but higher than amphibolites.

### 4.2 *Bouguer gravity anomaly*

The analysis of gravity data is effective in extrapolating the small and sparse geological information into the regional scale and to infer about depth persistence of the geological attributes. The
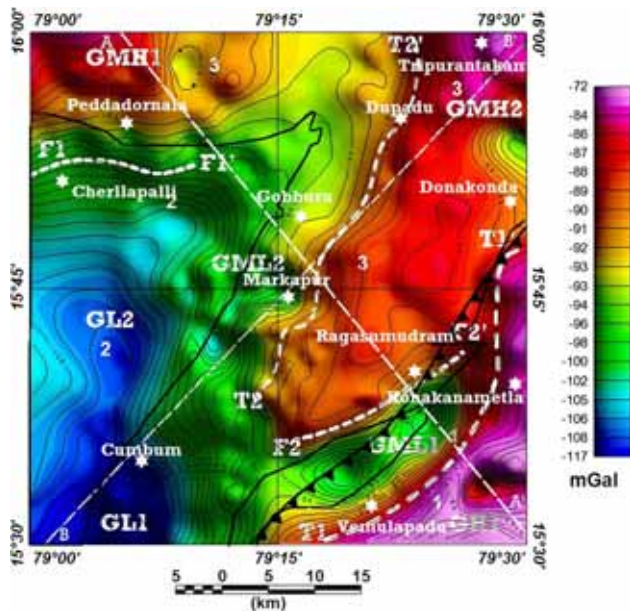


Figure 5. Bouguer gravity anomaly map; see text for details; GL1 and GL2: low gravity; GML1 and GML2: moderate to low gravity; GMH1 and GMH2: moderate to high gravity; T1–T1′: thrust delineated from gravity study; T2–T2′: inferred contact; F1–F1′: inferred fault. 1: Nellore Schist Belt (NSB); 2: Baironkonda Formation; 3: Cumbum Formation. Profiles A–A′ and B–B′ have been selected for study of gravity–magnetic responses. Gravity–magnetic joint modelling has been carried out along profile A–A′.

Bouguer gravity map along with contours is shown in figure 5. The map shows a total variation of 46 mGals with the amplitude ranging from –117 to –71 mGal. Based on the pattern of Bouguer gravity contours, some distinct features have been observed (figure 5). A prominent gravity high zone (GH1) separating the moderately low gravity zone (GML1) with steep gravity gradient contours is observed in the southeastern part of the study area (figure 5). The steep gradient is marked in the figure by a white line that mimics the trend and spatial location of the geologically reported thrust. This gradient zone is delineated as a thrust T1–T1′. The gravity values in the right-hand part (GH1) of the thrust T1–T1′ varies from $\sim -84$ to –71 mGals. The gravity high may be attributed to change in basement characteristics in terms of density, i.e., the basement below GH1 is of higher density. The left-hand part of thrust T1–T1′ has been marked as GML1. Geologically, it represents Baironkonda formation with gravity anomaly variation of approximately –104 to –95 mGal. The amplitude of the gravity anomaly and wavelength of the anomaly suggest that sediments are deposited in a graben-like structure.

The gravity high anomaly zone stretching from Ragasumudram to Tiruvantakam has been marked as GMH2, which is the second prominent feature in the Bouguer gravity anomaly map. The gravity value in this area varies from –92 to –82 mGal. This zone mainly covers Cumbum Formations. The western part of this zone indicates a moderate gradient (T2–T2′) with NE–SW trending gravity contours, which suggest contact of two litho-units. It probably indicates the contact of the low-density felsic basement and high-density mafic basement underneath the sediments. The relatively long wavelength anomaly of GMH2 indicates the deeper causative source. Denser basement may be the causative source.

The low gravity anomaly zone, encompassing GL1 and GL2 trending N–S direction, occurs over quartzite and shale of Baironkonda Formation. The gravity anomaly varies from –117 to –108 mGal over GL1, and over GL2, it ranges from –108 to –95 mGal. The low gravity anomaly closure over GL1 and GL2 may be attributed by granitic intrusive within the basement. We know the lateral variation in the density of the rock produces gravity anomaly. For the present case, average density of the sedimentary rocks (quartzite and limestone) are similar (table 1). So, the low density intrusive within the basement will be the

predominant contributor for the gravity low. The wavelength of the anomaly ($\sim 20$ km) also suggest causative source for the low at basement level. But the thickness of the sediment may also be contributing factor. Further, E–W trend of gravity contours is observed in the north of Cherllapalli and south of Peddadornala with a moderate gradient. This E–W trending feature is inferred to be a structural fault (F1–F1′) separating moderate gravity high GMH1 in the north and GL2 in the south. Rock samples with higher density values have been found over GMH1. These gravity values may be attributed due to the occurrence of high-density litho-units or due to gravity faulting with the northern part as an upthrown block.

### 4.3 *Magnetic anomaly map*

The RTE filter was applied on the Total Magnetic Intensity (TMI) grid and the resultant anomaly map is produced in figure 6. Some distinct anomaly zone can be identified from the RTE map. The anomaly zone, M–I, at the southern part of the study area is a prominent low, which indicates the presence of magnetic minerals in the sediments, but wavelength suggests that the causative source
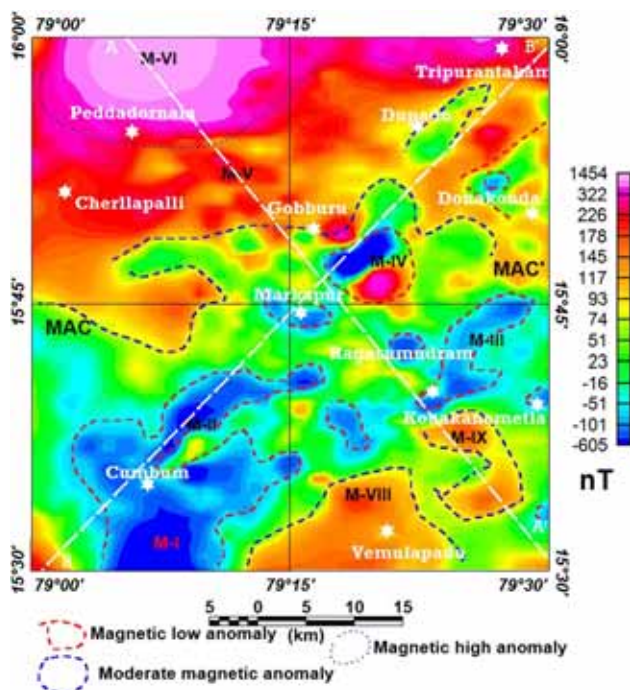


Figure 6. Magnetic anomaly map after applying RTE filter. 1: Nellore Schist Belt (NSB); 2: Baironkonda Formation; 3: Cumbum Formation. Profiles A–A′ and B–B′ have been selected for study of gravity–magnetic responses. Gravity–magnetic joint modelling has been carried out along profile A–A′.

is deeper. Another high magnetic anomaly zone M–VI at northern part suggests the presence of a rock unit with diamagnetic properties. There are other moderate frequency anomalies with low and high amplitude, which are marked in figure 6. In general, northern part of the study area is dominated by moderate to high magnetic anomalies. Similarly, southeastern part is dominated by moderately high anomalies. A conspicuous magnetic low to moderately low zone runs almost NE–SW direction from Cumbum to Donakonda. The change in moderately high anomaly to moderately low anomaly across MAC–MAC′ possibly indicates the change of basement characteristic in terms of magnetic property.

### 4.4 *Spectral analysis of gravity and magnetic data*

The power spectrums for both gravity and magnetic data are shown in figure 7. Two linear slope segments have been delineated from gravity spectrum (figure 7a) with depth to the interfaces at 4.8 and 1.4 km, respectively. Similarly, the magnetic spectrum (figure 7b) also shows two linear slope segments delineating depths to the magnetic interfaces at 4.2 and 1.4 km, respectively. The density and magnetic interface near 4.2 or 4.8 km possibly indicate the mean average depth to the basement. The interface at 1.4 km possibly indicates the mean depth of some high-density units such as rock units of NSB.

### 4.5 *Regional and residual gravity anomaly*

The amplitude and geometry of Bouguer Gravity Anomaly (BGA) are the cumulative contributions from different sources at different depths and physical contrast between the source body and surrounding. Residual and regional data separation of gravity anomalies has been carried out to delineate short wavelength anomaly from long wavelength regional features. The purpose of the residual map is to explain gravity highs and lows in terms of exposed geological features and also in defining the subsurface geometry of the exposed geological units. The residual anomaly map enhances the short wavelength/high frequency caused by shallow and local features. Whereas, the regional anomaly map enhances the long wavelength/low-frequency, which origantes from dipper and regional features. Different techniques are

Figure 7. Radial averaged power spectrum derived from (**a**) gravity data and (**b**) magnetic data.



Figure 8. Regional gravity map derived by applying low-pass filter to the Bouguer gravity map. GRL: Gravity Regional Low; GRM: Gravity Regional Moderate; GRMH: Gravity Regional Moderately High. Profiles A–A′ and B–B′ have been selected for study of gravity–magnetic responses. Gravity–magnetic joint modelling has been carried out along profile A–A′.
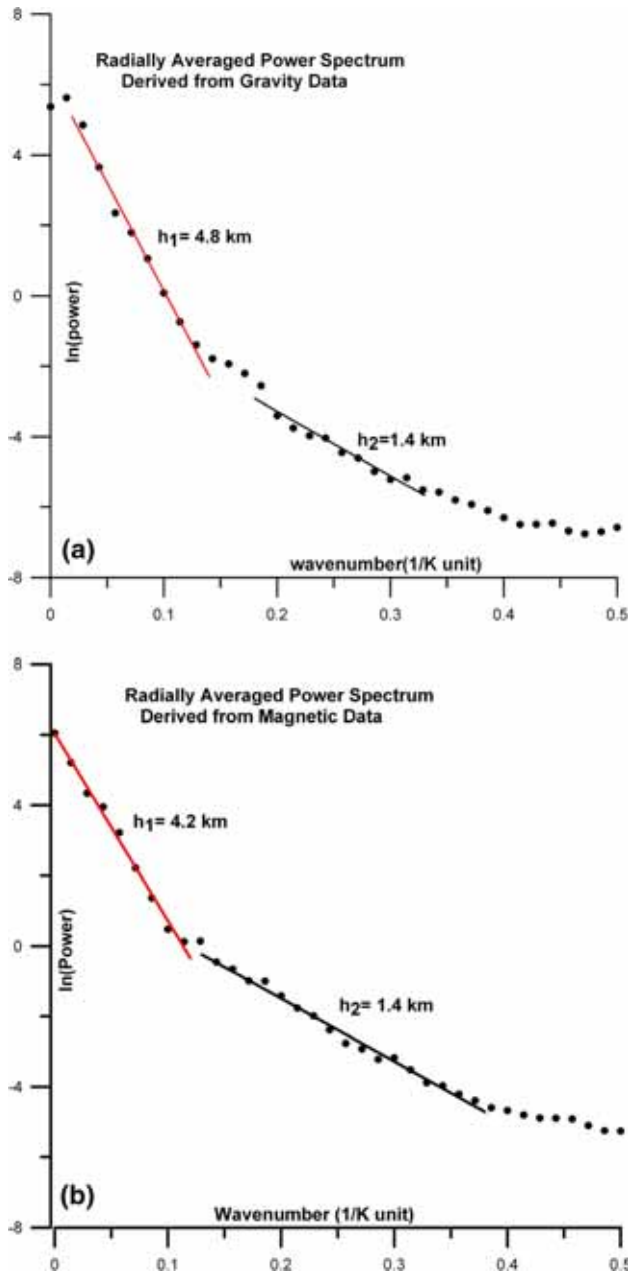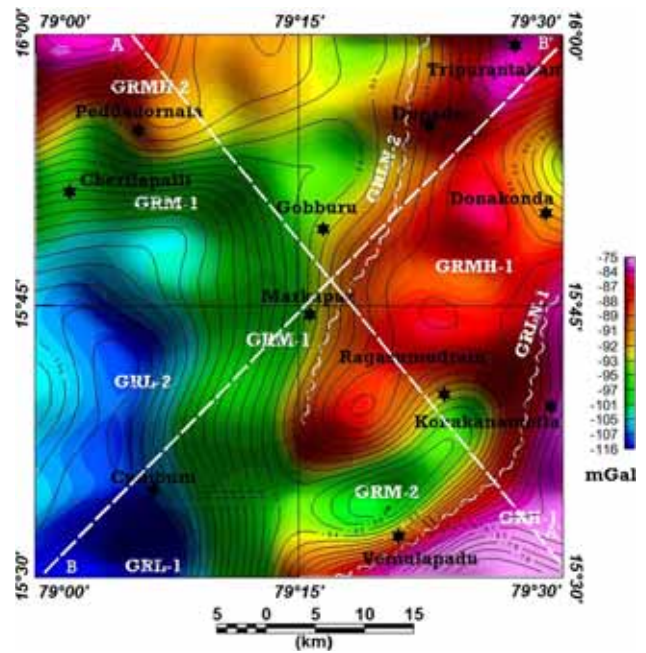
available for carrying out regional and residual separation of potential data, such as visual analysis, upward continuation, trend analysis and wavenumber analysis (Gupta and Ramani 1980; Mandal *et al.* 2015; Chowdari *et al.* 2017).

For the present study, regional component has been computed by applying low paas filter to the Bouguer gravity grid. The cut-off wavelength (12 km) for pass band was selected based on the spectral analysis of the data. The map (figure 8) shows moderate to high gravity anomaly (GRMH-1) in eastern part and moderate gravity anomalies

(GRM-1 and GRM-2) in central part and low gravity anomalies (GRL1 and GRL2) in SW part of the study area. There is a systematic increase of gravity values from SW to NE. It may suggest a change of the basement characteristic from silicic to mafic. The gravity linear zone GRL-2 may indicate litho contact separating silicic and mafic basement. At SE part, a NE–SW trending linear gradient zone (GRL-1) is observed. It may indicate a structural feature (fault/thrust). The southern part of GRL-1 is represented by high gravity zone (GRH-1) which may indicate contributions of high density rock units belonging to NSB and high density basement underneath of NSB. The regional gravity lows (GRL-1, GRL-2) can be attributed to granitic intrusion within the silicic basement. At northwestern corner, moderately high anomaly zone is observed which may indicate high density intrusion within the silicic basement.

The residual gravity data is computed by using a Butterworth bandpass filter. The cut-off frequencies are selected from the spectral analysis of the gravity data as 10 and 1 km. The residual gravity map (figure 9) expresses the contribution from shallower sources and its magnitude varies from
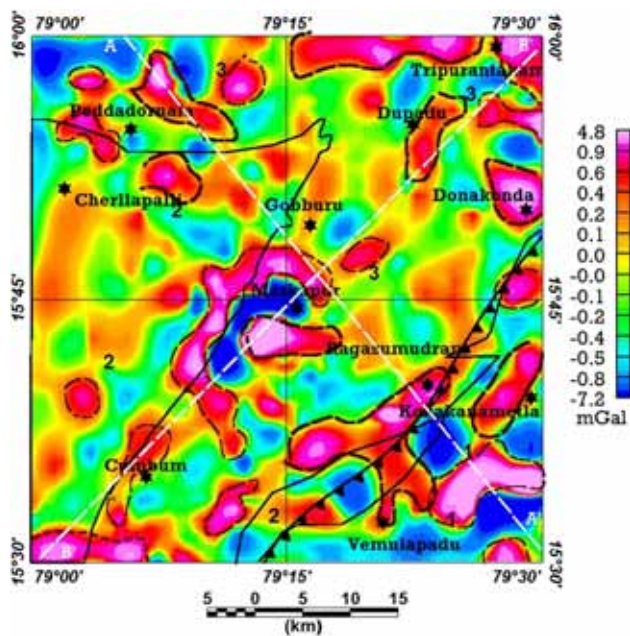
Figure 9. Residual gravity map. Residual gravity high zones are demarcated by black dotted line (see text for details). 1: Nellore Schist Belt (NSB); 2: Baironkonda Formation; 3: Cumbum Formation. Profiles A–A′ and B–B′ have been selected for study of gravity and magnetic responses. Gravity–magnetic joint modelling has been carried out along profile A–A′.



Figure 10. (**a**) Horizontal gradient of gravity grid. (**b**) Superimposed image of horizontal gradient of gravity data and geological map (50% transparency). 1: Nellore Schist Belt (NSB); 2: Baironkonda Formation; 3: Cumbum Formation.

–8 to 9 mGal. The residual gravity map shows numbers of high frequency low and high amplitude anomalies. The prominent gravity highs are marked in figure 9 by black dashed line as the residual gravity highs are important for sulphide mineralization or base metal exploration for the study area. A conspicuous residual gravity high at the northern and southern parts of Markapur seems to be prospectus zone for the mineral occurrence. It is well corroborated by density and susceptibility image. There are also some prominent highs in the southeastern part over NSB.

### 4.6 *Horizontal gradient of gravity data*

The horizontal gradient of gravity data has facilitated to demarcate lateral density inhomogeneities of shallow vertical extension. The boundaries of the moderate to high gradient zones are marked (figure 10a). The demarcated boundaries in many cases corroborate well with surface lithology. A correlation study with the geology map reveals that the boundaries of the high gradient zones corroborate well with exposed quartzites (figure 10b).
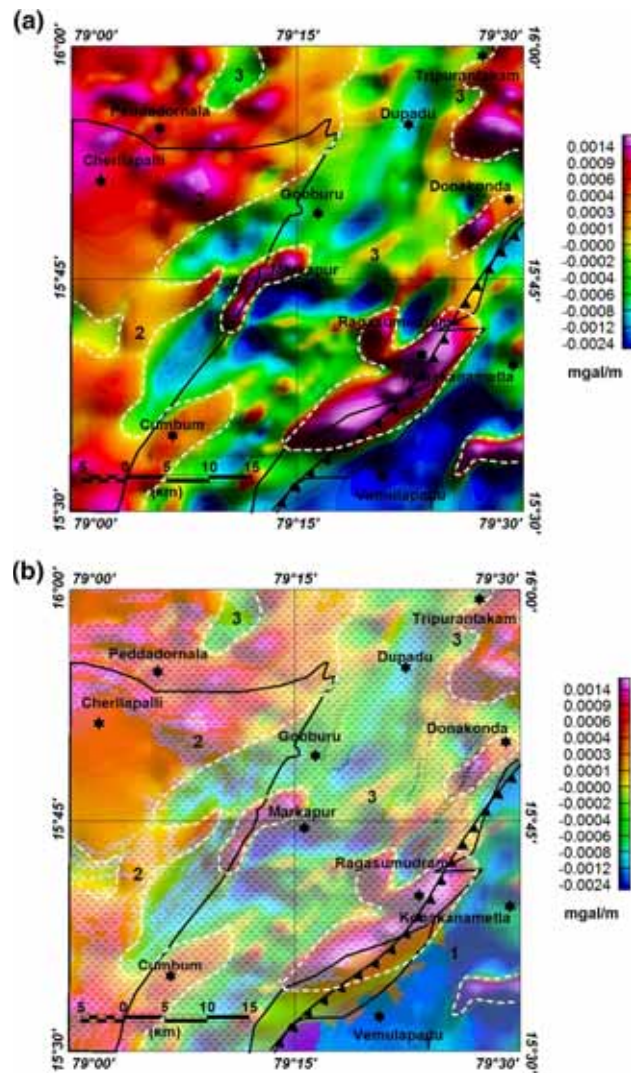
### 4.7 *Gravity and magnetic response along profiles A–A′ and B–B′*

Profiles A–A′ and B–B′ are selected to study the Bouguer gravity, residual gravity, regional gravity and RTE magnetic responses over different geological formations (figure 2). Gravity, residual gravity, regional gravity and RTE magnetic responses over the geological section along A–A′ and B–B′ are presented in figure 11.

The gravity values in profile A–A′ (figure 11a) show that total variation is from –99 to –73 mGal. A gravity low (GL-I) of ∼20 km wavelength is observed in NW part of the profile over quartzite and shale. The wavelength and pattern of the anomaly suggest that causative source is deeper, may be low density intrusive within the basement.
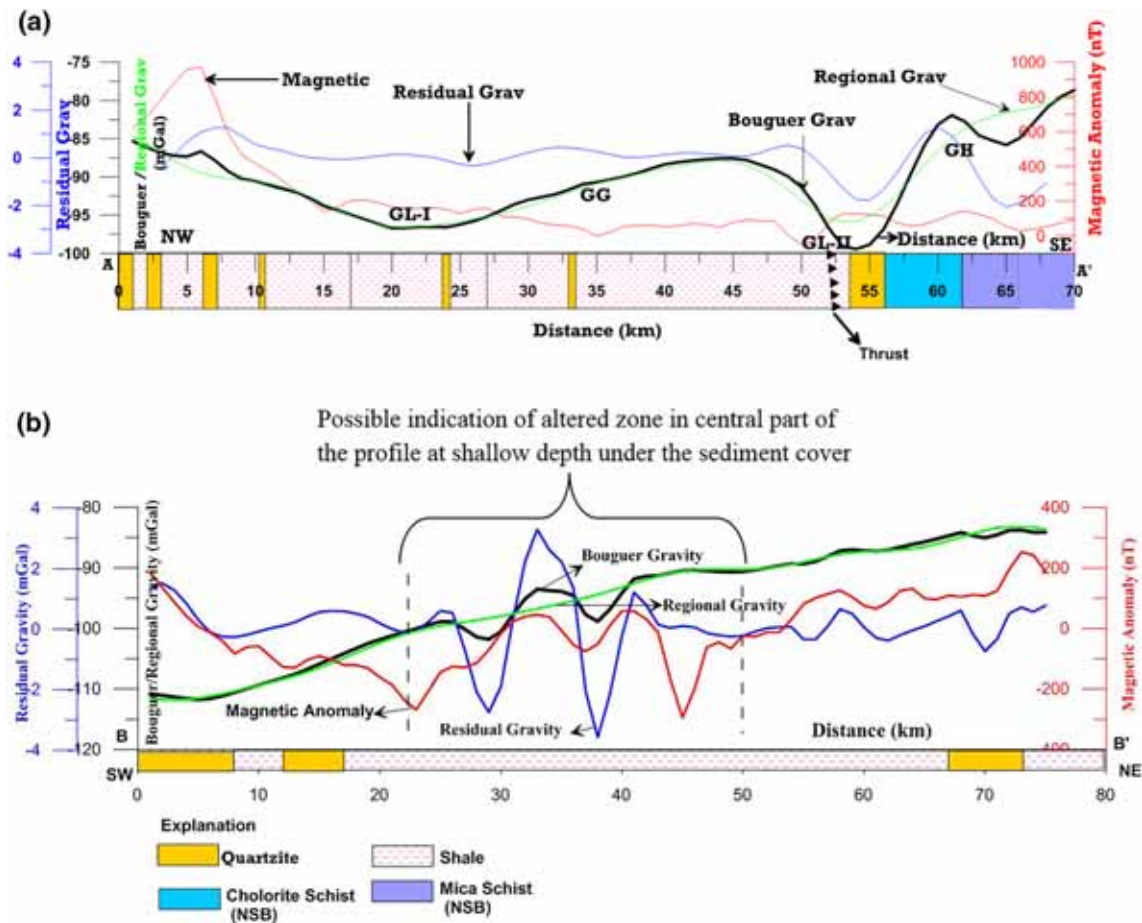
Figure 11. Gravity and magnetic responses over different geological formations along (**a**) profile A–A′ and (**b**) profile B–B′.

The gravity value increases with a moderate gradient (GG) in further SE direction. The moderate to high gravity is observed over NSB (GH). The second gravity low (GL-II) is of comparatively shorter wavelength, which is observed at the vicinity of the thrust zone. This low is reflected in both residual and regional components, which indicate extension of the causative source anomaly to deeper level. The prominent anomalies of Bouguer gravity profiles (GL-I, GL-II, GG and GH) are also reflected in regional gravity profile. It indicates that prominent anomalies are caused by sources at deeper depth. The overall increase of gravity value (both in Bouguer Gravity profile and Regional Gravity profile) towards SE part indicates change in basement characteristic terms of density and the probably gneissic basement is replaced by the mafic basement of EGMB Group of rocks. Magnetic profile anomaly does not register any conspicuous variation except at NW part, where a sharp rise is observed.

The gravity values in profile B–B′ (figure 11b) exhibit systematic increase of Bouger gravity value

from SW to NE with variation from –112 to –83 mGal. The regional gravity profile follows the same trend. It indicates major contributions to the Bouguer gravity is accounted by sources at deepr depth. Probably density variation within the basement made a major contribution to the Bouguer gravity profile. Central part of the profile marked within black dashed line (figure 11b) shows presence of high frequency component, which is corroborated with large variation in residual gravity field and RTE magnetic anomaly. It may indicate presence of altered zone in central part of the profile at shallow depth under the sediment cover.

### 4.8 *Joint gravity–magnetic modelling*

The crustal architecture, along profile A–A′ (figure 11a) running in NW–SE direction (figure 2), has been obtained by joint gravity–magnetic modelling. The profile orientation is appropriate to study the interface of CB and NSB as it cuts across the anomaly trends caused due to
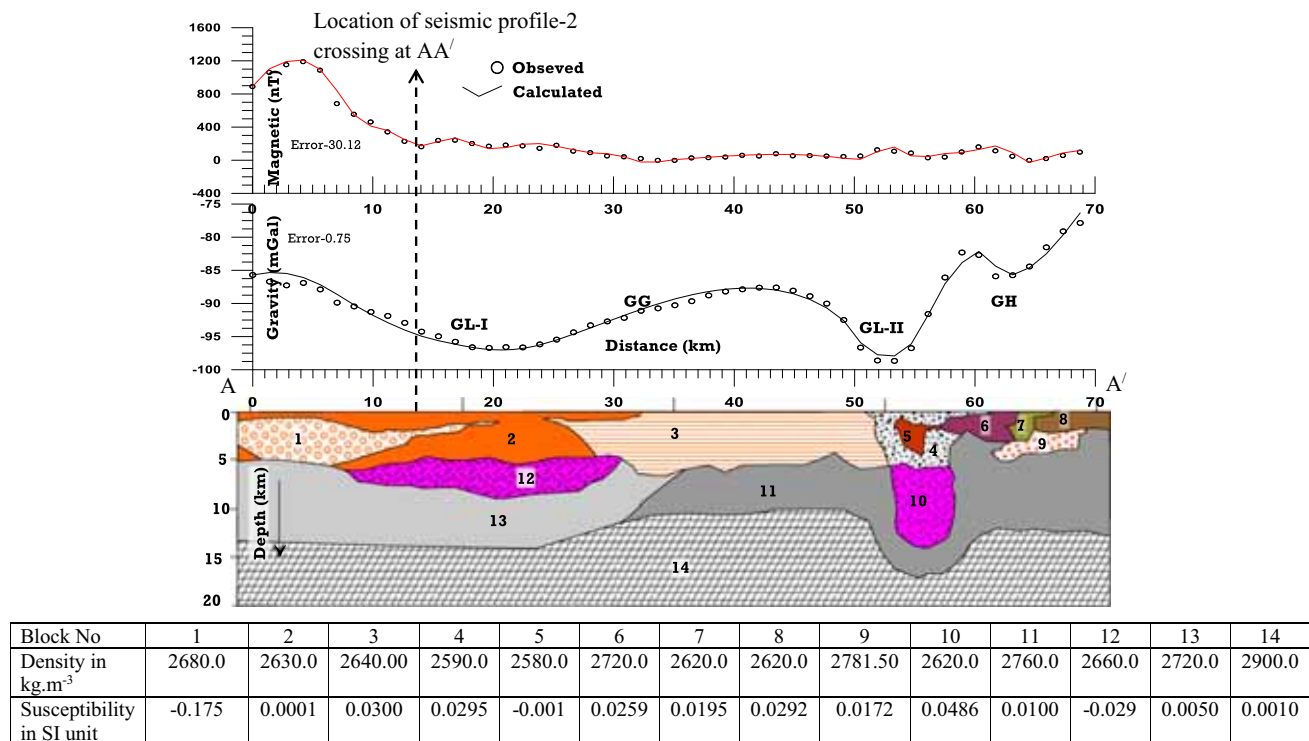
Figure 12. Joint gravity–magnetic model along profile A–A′. The model parameters for each block is provided in the legend.

| Block No | 1 | 2 | 3 | 4 | 5 | 6 | 7 | 8 | 9 | 10 | 11 | 12 | 13 | 14 |
|---|---|---|---|---|---|---|---|---|---|---|---|---|---|---|
| Density in kg.m⁻³ | 2680.0 | 2630.0 | 2640.00 | 2590.0 | 2580.0 | 2720.0 | 2620.0 | 2620.0 | 2781.50 | 2620.0 | 2760.0 | 2660.0 | 2720.0 | 2900.0 |
| Susceptibility in SI unit | -0.175 | 0.0001 | 0.0300 | 0.0295 | -0.001 | 0.0259 | 0.0195 | 0.0292 | 0.0172 | 0.0486 | 0.0100 | -0.029 | 0.0050 | 0.0010 |

major tectonic domains and geological formations. Generally, a crustal model derived using potential field data suffers from non-uniqueness. A joint gravity and magnetic modelling reduces the ambiguity and results in a more reliable crustal model, which can bring a new perspective to the geological understanding of the area (Ramadass *et al.* 2006; Radhakrishna *et al.* 2012; Hinze *et al.* 2013; Singh *et al.* 2014; Rao *et al.* 2018; Ganguli *et al.* 2019). To negate the non-uniqueness issue, further we tried to constrain the model from the results of seismic studies, spectral analysis of the gravity and magnetic data, measured density and susceptibility values of the rock samples. Here, initially, forward modelling has been performed using GM-SYS software (Geosoft Inc. 2004), assuming common source for both gravity and magnetic anomalies and by synergistically combining the information compatible with both the data sets. The crustal model was generated by forwarding modelling, which was iteratively modified to obtain a satisfactory fit to the observed gravity and magnetic data. Then the model parameters are jointly inverted using joint inversion routine available in the software (GM-SYS) to make small changes in the model parameters to obtain an optimal fit to the observed data. The computational algorithm of the joint

gravity–magnetic modelling of GM-SYS is derived from the methods of Talwani *et al.* (1959) and Talwani and Heirtzler (1964). The inversion is made using algorithm of Marquardt (1963). The software incorporates gravity–magnetic programs developed by the U.S. Geological Survey and also Semi-Automated Marquardt Inversion code (SAKI) (Webring 1985).

The profile runs in NW–SE direction for a length of 70 km (figure 12). Considering the length of the profile and wavelength of the anomalies, a crustal section of 20 km depth extension was selected for modelling. The initial crustal configuration is constrained from velocity depth section of Seismic Profile-2 (Kaila and Tewari 1985). Initially, we have fixed the upper crustal depth at $\sim$10 km according to the velocity–depth section. The seismic section provided by Chandrakala *et al.* (2013) shows a mid-crustal layer, which is characterized by a velocity of 6.4 km/sec. The corresponding density value is 2900 kg m⁻³ following the equation $d = 0.541 + 0.3601\,V_p$ (Christensen and Mooney 1995). The formula was derived for crystalline crustal rocks. Singh and Mishra (2002) derived basement density as 2750 kg m⁻³ from linear optimization of velocity–density relationship provided by Barton (1986). So, the initial basement density was assumed as 2750 kg m⁻³. The

density of upper crustal sedimentary unit was assigned in consultation with the measured density value of different rocks. The susceptibility values for the upper crustal layer were initially considered between 0.0002 and 0.00001 SI units based on the measured susceptibility values of the rocks samples. However, later on, both density and susceptibility values were calibrated for minimizing the error between the observed and calculated anomaly.

A careful observation of the gravity profile shows a moderate gravity gradient at the SE portion of the profile. It is more prominent in regional profile (figure 11a) and high-frequency signals are superimposed on this trend. The gradient is interpreted in terms of change of basement characteristic underneath the sediments. The model shows (figure 12) that the basement (block-13), at NW part of the profile, is characterized by a litho-unit with density (D) 2720 kg m$^{-3}$ and susceptibility (S) 0.005 SI. It is replaced by denser litho-unit (block 11) of mafic nature towards SE part of the profile. This implicates a change in the nature of basement characteristics and silicic (granitic–gneissic) basement in NW part is replaced by mafic basement (charnockitic) in the SE part. The gravity low 'GL-I' is attributed by low density intrusive (block-12, probably granitic) within the basement overlaid by low-density sediments (block-2). The short wavelength low gravity anomaly (GL-II) is caused by low density litho-unit (blocks 4 and 5) lying over another low density litho-unit (block-10) probably granitic rock. The magmatic activity as indicated by granitic intrusion within the basement might have triggered extensional regime and graben like structure was created upon which sedimentation took place. Comparatively lower density of the sediments may be indicating shaley nature of the sediments. The litho-unit extends up to $\sim$6.0 km depth.

In the north-western part of the profile, the magnetic high associated with moderate gravity high (GMH-I) indicates the presence of moderate density (*D*: 2680 kg m$^{-3}$) litho-unit of diamagnetic nature (*S*: –0.174 SI). It probably indicates the presence of quartzite. The gravity gradient (GG) is accounted by a sedimentary unit of mafic nature and change in underneath basement density. The SE part of the profile shows the presence of an assemblage of moderate to high-density litho-units of mafic character. The assemblage represents Nellore Schist Belt (NSB). The model further

shows the occurrence of shallow mafic basement underneath NSB.

## 5. Discussions

The regional geotectonic feature of the study area includes eastern part of CB and Nellore Schist Belt (NSB). It is generally believed that CB is conspicuously bounded by two deep seated fault filled with succession of igneous and Proterozoic rock that rest over granitic–gneissic basement (Saha and Tripathy 2012; Pandey *et al.* 2018). The upper crustal model derived from the joint gravity–magnetic modelling has provided new insights on the nature and geometery of sedimentary rocks and underneath basement. The regional gravity map (figure 8) shows that there is a systematic increase in Bouguer gravity values from west to east. It indicates the change in basement characteristics. The modelling indicates silicic basement in NW part, which is replaced by mafic basement in SE part of the study area. The systematic increase of gravity value towards the east also indicates a decrease in basement depth. Most of the velocity sections across eastern margin of CB clearly indicates thick sediments below the Nallamalai Fold Belt (NFB, Kaila *et al.* 1979; Kaila and Tewari 1985; Chandrakala *et al.* 2015) overlying the granitic gneiss basement of Dharwar, while the basement is shallow and of mafic beneath the NSB due to upthrusting of higher velocity and higher density lower crustal material at shallow depth. The present study indicates possible occurrence of high-density EGMB crust below the eastern fringe of CB. The eastern fringe of CB is geologically marked as NSB. So, our study indicates possible occurrence of EGMB crust under the cover of NSB. The seimic velocity structure along seimic profile-2 (Kaila and Tiwari 1985) indicates eastward dip below NSB and up-thrusted feature below EGMB. The eastward dip is not evident in our gravity–magnetic model, but the contact of silicic and mafic basement appears to be faulted and may indicate up-thrusted basement of EGMB.

The CB is a sedimentary-volcanic sequence composed of sediments, both intrusive and extrusive igneous bodies. Compressional and extensional tectonics are attributed for the development of the basin (Chetty 2011; Mishra 2011; Chandrakala *et al.* 2013). The southwestern part of the regional gravity map (figure 8) is characterized by gravity low and it indicates possible occurrence of a

granitic intrusive rock unit. The CB is character-ized by intermittent magmatic activity; however, subaerial basaltic lavas and sills of Paleoprotero-zoic age parallel to the margin are only exposed in the western part of the CB (Anand *et al.* 2003). Reported age of granitic intrusives in the eastern margin of Nallamalai Fold Belt (NFB) is 1584 Ma (Crawford and Compston 1973; Saha and Chak-raborti 2007). The granitic body as evinced by the regional gravity map may be of the same age. The gravity contour pattern over the gravity low (figure 5) perturbs the NE–SW trending contour associated with thrusted contact of NSB–NFB. It implies that the age of the intrusive is younger than the thrust. So, our study shows evidence of mag-matic activity well within and underneath the CB, which may have played a role in the evolution of the basin. The granitic intrusive within the base-ment indicates repeated magmatism in the area. The absence of silicic upper crust in SE part of the study area and repeated magmatism indicate that the area was subjected to a deep-seated thermal anomaly (Mall *et al.* 2008; Chandrakala *et al.* 2015).

The previous geophysical model derived from gravity and seismic data across CB revelaed homogeneous nature of Cuddapah sediments (Singh and Mishra 2002; Chandrakala *et al.* 2015) in terms of density and seismic velocity. The 2-D gravity modelling constrained from newly available seismic velocity structure across CB was carried out by Pandey *et al.* (2018). The model shows density of Cuddapah sediments varies from 2550 to 2690 kg m$^{-3}$. The present study with joint grav-ity–magnetic modelling reveals that nature of Cuddapah sediments varies both in terms of den-sity and magnetic property. The basement depth varies considerably from ∼1.5 to ∼6.5 km. The seismic study by Chandrakala *et al.* (2015) indi-cated maximum thickness of the Cuddapah sedi-ments as ∼4.0 km. The present study indicates more thickness of the sediments.

We have tried to make a corroborative study based on gravity and magnetic anomalies. The boundaries of the different anomalies delineated from different data source have been placed in the same figure to generate a composite map (figure 13). It is found in many cases that the boundaries of residual gravity high (RGH) and magnetic (RTE) anomalies have very good cor-roboration. The magnetic anomaly zone M-I and M-II (figure 6) encompasses RGH (figure 9). However, RGH at north and western part of
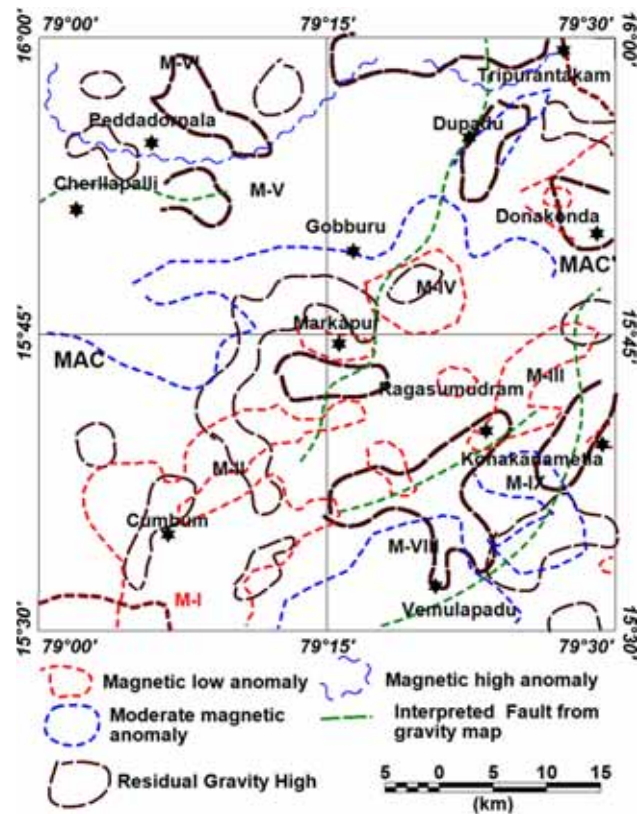


Figure 13. Composite map showing structure and boundaries of residual high gravity anomalies and magnetic anomaly delineated from gravity and magnetic data. MAC–MAC': curvilinear feature has inferred which depicts change magnetic property of the basement.

Markapur is not associated with a magnetic anomaly. The magnetic anomaly zone M-IV (figure 6) is associated with RGH (figure 9). Mag-netic moderate zone M-VIII and M-IX are encom-passing RGH. The magnetic and gravity anomaly pattern suggest that area encompassed by M-II and M-II is a potential zone for sulphide mineralization or base metals.

## 6. Conclusions

The study shows that gravity magnetic survey has provided significant insights into the shallow crustal architecture and tectonics of the eastern margin of CB. The thrusted contact of NSB and Cuddapah sediments has been well delineated in the gravity map. The moderate to high Bouguer gravity anomaly zones in eastern and southeastern parts of the study area are attributed to the mafic basement. It indicates that the mafic basement (EGMB) is probably extended beneath the Cud-dapah sediments. The study area had experienced both compressional and extensional tectonics as

well as magmatic activity. The horizontal gradient map has enabled to delineate the contacts of litho-units of shallow occurrence. Through residual gravity analysis, high density concealed rocks are delineated. The integrated study shows a good corroboration of residual gravity with magnetic anomalies. Based on this study, the area surrounding Cumbum has been identified for mineral investigation. A conspicuous residual gravity high at the northern and southern parts of Markapur seems to be prospective zone for the mineral occurrences. From the interpretation of gravity–magnetic maps some new structural features have also been delineated.

## Acknowledgements

## References

Anand M, Gibson S, Subba Rao V, Keelly S P and Dickin A P 2003 Early Proterozoic melt generation process beneath the intra-cratonic Cuddapah Basin, southern India; *J. Petrol.* **44(12)** 2139–2172.

Barton P J 1986 The relationship between seismic velocity and density in the continental crust – a useful constraint? *Geophys. J. Roy. Astron. Soc.* **87** 195–206.

Chandrakala K, Mall D M, Sarkar D and Pandey O P 2013 Seismic imaging of the Proterozoic Cuddapah basin, south India and regional geodynamics; *Precamb. Res.* **213** 277–289.

Chandrakala K, Pandey O P, Prasad A S S S R S and Sain K 2015 Seismic imaging across the Eastern Ghats Belt–Cuddapah Basin collisional zone, southern Indian Shield and possible geodynamic implications; *Precamb. Res.* **271** 56–64.

Chetty T R K 2011 Tectonics of Proterozoic Cuddapah Basin, southern India: A conceptual model; *J. Geol. Soc. India* **78** 446–456.

Chetty T R K and Murthy D S N 1994 Collision tectonics in the late Precambrian Eastern Ghats Mobile Belt: Mesoscopic to satellite-scale structural observations; *Terra Nova* **6(1)** 72–81.

Chouhan A K, Singh D, Pal S K and Choudhury P 2020 Delineation of subsurface geological fractures in the Cambay rift and surrounding regions of NW India: An integrated approach using satellite derived EIGEN-6C4 gravity data; *Geocarto Int.*, https://doi.org/10.1080/10106049.2020.1716395.

Chowdari S, Singh B, Rao B N, Kumar N, Singh A P and Chandrasekhar D V 2017 Structural mapping based on potential field and remote sensing data, South Rewa Gondwana Basin, India; *J. Earth Syst. Sci.* **126** 84.

Christensen N I and W D Mooney 1995 Seismic velocity structure and composition of the continental crust: A global view; *J. Geophys. Res.* **195(100)** 9761–9788.

Crawford A R and Compston W 1973 The age of the Cuddapah and Kurnool systems, southern India; *J. Geol. Soc. Australia* **19(4)** 453–464.

Dasgupta S, Bose S and Das K 2013 Tectonic evolution of the Eastern Ghats Belt, India; *Precamb. Res.* **227** 247–258.

Dharma Rao C V and Reddy U V B 2009 Petrological and geochemical characterization of Proterozoic ophiolitic mélange, Nellore–Khammam schist belt, SE India; *J. Asian Earth Sci.* **36** 261–276.

Dobmeier C J and Raith M M 2003 Crustal architecture and evolution of the Eastern Ghats belt and adjacent regions of India; In: *Proterozoic East Gondwana: Supercontinent Assembly and Breakup* (eds) Yoshida M, Windley B F and Dasgupta S; *Geol. Soc. London, Spec. Publ.* **206** 145–168.

Dobrin M B and Savit C H 1988 *Introduction to Geophysical Prospecting*; McGraw-Hill Book Company, ISBN 0-07-100404-1.

Fountain D M and Salisbury M H 1981 Exposed cross-sections through the continental crust: Implications for crustal structure, petrology, and evolution; *Earth Planet. Sci. Lett.* **56** 263–277.

Ganguli S S, Singh S, Das N, Maurya D, Pal S K and Rama Rao J V 2019 Gravity and magnetic survey in south western part of Cuddapah Basin, India and its implication for shallow crustal architecture and mineralization; *J Geol. Soc. India* **93(4)** 419–430.

GM-SYS 2004 Geophysical Processing and Analysis module of Geosoft, Inc.

GSI-NGRI 2006 Gravity Anomaly Map of India on 1:2 Million Scale. Geological Survey of India, Hyderabad, and National Geophysical Research Institute, Hyderabad, India; *Maps* 1–13.

Gibb R A and Thomas M D 1976 Gravity signature of fossil plate boundaries in the Canadian Shield; *Nature* **262 (5565)** 199.

Gibb R A, Thomas M D, Lapointe P L and Mukhopadhyay M 1983 Geophysics of proposed Proterozoic sutures in Canada; *Precamb. Res.* **19(4)** 349–384.

Gupta V K and Ramani N 1980 Some aspects of regional residual separation of gravity anomalies in a Precambrian terrain; *Geophysics* **45** 1412–1426.

Hinze W J, Von Frese R R and Saad A H 2013 *Gravity and magnetic exploration: Principles, practices, and applications*, Cambridge University Press.

Jayananda M, Moyen J F, Martin H, Peucat J J, Auvray B and Mahabaleswar B 2000 Late Archaean (2550–2520 Ma) juvenile magmatism in the Eastern Dharwar craton, southern India: Constraints from geochronology, Nd–Sr isotopes, and whole rock geochemistry; *Precamb. Res.* **99(3–4)** 225–254.

Kaila K L, Chowdhury K R, Reddy P R, Krishna V G, Narain H, Subbotin S I, Sollogub V B, Chekunov AV, Kharetchko G E, Lazarenko M A and Ilchenko T V 1979 Crustal structure along Kavali–Udipi profile in the Indian peninsular shield from deep seismic sounding; *J. Geol. Soc. India* **20** 307–333.

Kaila K L and Tewari H C 1985 Structural trends in the Cuddapah basin from deep seismic soundings (DSS) and their tectonic implications; *Tectonophys.* **115 (1–2)** 69–86.

Kailasam L N 1976 Geophysical studies of the major sedimentary basins of the Indian craton, their deep structural features and evolution; *Tectonophys.* **36(1–3)** 225–245.

Kesavamani M, Rao N B K and Rama Rao J V 1997 Characteristics of granite greenstone basement below the Cuddapahs: A geophysical insight; *J. Geophys. Union* **6** 27–29.

Krishna Brahmam N 1989 Gravity and seismicity of the Cuddapah basin and surrounding places; *J. Geol. Soc. India* **34** 373–384.

Kumar U, Narayan S and Pal S K 2019 New insights on structure and tectonics over the Laxmi Ridge using EIGEN-6C4 modelled gravity data; *Ind. J. Geo Marine Sci.* **48(12)** 1999–2005.

Kumar U, Pal S K, Sahoo S D, Narayan S, Saurav, Mondal S and Gunguli S S 2018 Lineament mapping over Sir Creek offshore and its surroundings using high resolution EGM2008 Gravity data: An integrated derivative approach; *J. Geol. Soc. India* **91(6)** 671–678.

Mall D M, Pandey O P, Chandrakala K and Reddy P R 2008 Imprints of a Proterozoic tectonothermal anomaly below the 1.1 Ga kimberlitic province of southwest Cuddapah Basin, Dharwar Craton (southern India); *Geophys. J. Int.* **172** 422–438.

Mandal A, Gupta S, Mohanty W K and Misra S 2015 Subsurface structure of a craton–mobile belt interface: Evidence from geological and gravity studies across the Rengali Province–Eastern Ghats Belt boundary, eastern India; *Tectonophys.* **662** 140–152.

Manikyamba C, Kerrich Robert, Ignacio Gonzalez-Alvarez, Mathur R and Khanna T C 2008 Geochemistry of Paleoproterozoic black shales from the intracontinental Cuddapah basin, India: Implications for provenance, tectonic setting, and weathering intensity; *Precamb. Res.* **162** 424–440.

Marquardt D W 1963 An algorithm for least squares estimation of non-linear parameters; *J. Soc. Ind. Appl. Math.* **11** 431–441.

Mishra D C 2011 *Gravity and Magnetic Methods for Geological Studies*; BS Publications, CRC Press, Hyderabad, USA, 938p.

Murthy Y G K 1981 The Cuddapah Basin – A review of basin development and basement framework relations; Fourth workshop on *Status, Problems and Programmes in Cuddapah basin,* Institute of Indian Peninsular Geology, Hyderabad, pp. 51–73.

Pal S K and Kumar S 2019 Subsurface structural mapping using EIGEN-6C4 data over Bundelkhand craton and surroundings: An appraisal on kimberlite/lamproite emplacement; *J. Geol. Soc. India* **94(2)** 188–196.

Pal S K, Vaish J, Kumar S and Bharti A K 2016 Coalfire mapping of East Basuria Colliery, Jharia coal field using Vertical Derivative Technique of Magnetic data; *J. Earth Syst. Sci.* **125(1)** 165–178.

Pal S K, Vaish J, Kumar S, Priyam P, Bharti A K and Kumar R 2017 Downward continuation and Tilt Derivative of magnetic data for delineation of concealed coal fire in East Basuria Colliery, Jharia coal field, India; *J. Earth Syst. Sci.* **126(53)** 1–17.

Pandey O P, Chandrakala K, Vasanthi A and Kumar K S 2018 Seismically imaged shallow and deep crustal structure and potential field anomalies across the Eastern Dharwar Craton, south Indian shield: Possible geodynamical implications; *J. Asian Earth Sci.* **157** 302–316.

Radhakrishna M, Twinkle D, Nayak S, Bastia R and Rao G S 2012 Crustal structure and rift architecture across the Krishna–Godavari basin in the central Eastern Continental Margin of India based on analysis of gravity and seismic data; *Mar. Petrol. Geol.* **37(1)** 129–146.

Ram Babu H V 1993 Basement structure of the Cuddapah Basin from gravity anomalies; *Tectonophys.* **223** 411–422.

Ramadass G, Rao I R and Himabindu D 2006 Crustal configuration of the Dharwar craton, India, based on joint modelling of regional gravity and magnetic data; *J. Asian Earth Sci.* **26(5)** 437–448.

Rao G S, Kumar M and Radhakrishna M 2018 Structure, mechanical properties and evolution of the lithosphere below the northwest continental margin of India; *Int. J. Earth Sci.* **107(6)** 2191–2207.

Saha D and Chakraborti S 2007 Advective heat transfer and fabric development in a shallow crustal intrusive granite – the case of Proterozoic Vellaturu granite, south India; *J. Earth Syst. Sci.* **116(5)** 433–450.

Saha D, Chakraborty S and Tripathy V 2010 Intracontinental thrusts and inclined transpression along eastern margin of the Dharwar craton, India; *J. Geol. Soc. India* **75** 323–337.

Saha D and Tripathy V 2012 Paleoproterozoic sedimentation in the Cuddapah basin, south India and regional tectonics: A review; In: *Paleoproterozoic of India* (eds) Mazumder R and Saha D, *Geol. Soc. London, Spec. Publ.* **365(1)** 161–184, https://doi.org/10.1144/SP365.2.

Saha D and Patranabis-Deb S 2014 Proterozoic evolution of Eastern Dharwar and Bastar cratons, India – an overview of the intracratonic basins, craton margins and mobile belts; *J. Asian Earth Sci.* **91** 230–251.

Saha D, Sain A, Nandi P, Mazumder R and Kar R 2015 Tectonostratigraphic evolution of the Nellore schist belt, southern India, since the Neoarchaean; *Geol. Soc. London, Memoirs* **43(1)** 269–282.

Sahoo S D and Pal S K 2019 Mapping of structural lineaments and fracture zones around the Central Indian Ridge (10°–21°S) using EIGEN-6C4 Bouguer gravity data; *J. Geol. Soc. India* **94(4)** 359–366.

Singh A P and Mishra D C 2002 Tectono sedimentary evolution of Cuddapah basin and Eastern Ghats mobile belt (India) as Proterozoic collision: Gravity, seismic and geodynamic constraints; *J. Geodyn.* **33** 249–267.

Singh B, Rao M P, Prajapati S K and Swarnapriya C 2014 Combined gravity and magnetic modelling over Pavagadh and Phenaimata igneous complexes, Gujarat, India: Inference on emplacement history of Deccan volcanism; *J. Asian Earth Sci.* **80** 119–133.

Smithson S B 1971 Densities of metamorphic rocks; *Geophysics* **36(4)** 690–694.

Spector A and Grant F S 1970 Statistical methods for interpreting aeromagnetic data; *Geophysics* **35** 293–302.

Subrahmanyam C and Verma R K 1982 Gravity interpretation of the Dharwar greenstone-gneiss-granite terrain in the southern Indian shield and its geological implications; *Tectonophys.* **84(2–4)** 225–245.

Talwani M and Heirtzler J R 1964 Computation of magnetic anomalies caused by two dimensional bodies of arbitrary shape; In: *Computers in the mineral industries* (ed.) Parks G A, Part 1, vol. 9, Stanford University Publications, Geological Sciences, pp. 464–480.

Talwani M, Worel J L and Landisman M 1959 Rapid gravity computations for two-dimensional bodies with application to the Mendocino submarine fracture zone; *J. Geophys. Res.* **64** 49–59.

Tripathy V and Saha D 2013 Plate margin paleostress variations and intracontinental deformations in the evolution of the Cuddapah basin through Proterozoic; *Precamb. Res.* **235** 107–130.

Thomas M D, Grieve R A F and Sharpton V L 1992 Structural fabric of the North American continent, as defined by gravity trends; In: *Basement tectonics* (ed.) Mason R, Vol. 7, Kluwer Academic Press, pp. 257–276.

Vijaya Kumar K, Ernst W G, Leelanandam C, Wooden J L and Grove N J 2010 First Paleoproterozoic ophiolite from Gondwana: Geochronologic–geochemical documentation of ancient oceanic crust from Kandra, SE India; *Tectonophys.* **487** 22–32.

Webring M W 1985 SAKI: A Fortran program for generalized linear inversion of gravity and magnetic profiles; USGS Open File Rep 85–12 104.